The 2013 World Congress on
Advances in Structural Engineering and Mechanics (ASEM13)
Jeju, Korea, September 8-12, 2013

CFD simulation of Vortex-Induced Vibration with change in cylinder array

Tae-Jin Kang[1)] and Warn-Gyu Park[1)*]

[1)]*School of Mechanical Engineering, Pusan National University, Busan 609-735, Korea*

ABSTRACT

The dynamic behavior of a structure is displayed in many engineer applications. In particular, the phenomenon of Vortex-Induced Vibration (VIV) in a floating body system plays a key role in the design of substructures such as marine cables and subsea pipelines. In this study, we conducted a CFD simulation of the dynamic response of an array of cylinders. To simulate a two-dimensional incompressible viscous flow, the present study uses ANSYS FLUENT based on the finite volume method. The cylinder is free to oscillate with multiple degrees of freedom in a uniform flow. The motion of the cylinder is modeled using a damped degree of freedom system. First, the drag coefficient of a single cylinder is compared to the value obtained through experimental results when the Reynolds number is 200. In addition, the Strouhal number is compared to the value obtained in experimental results, but the Reynolds number is changed. Next, studies are conducted using cylinders arranged in a series. The center-to-center distance between two cylinders is 2.5 D.

1. Introduction

The dynamic behavior of a structure is displayed in many engineer applications. In particular, the phenomenon of Vortex-Induced Vibration (VIV) in a floating body system plays a key role in the design of substructures such as marine cables and subsea pipelines. This VIV causes a phenomenon called “lock-in.” The lock-in phenomenon indicates that simultaneous vibrations between the vortex and vibration frequencies are a characteristic of the fluid-structure interaction. When a lock-in occurs, the oscillation frequency in the cross-stream direction becomes twice the frequency in the streamwise direction. At this time, the substructure is forced to oscillate sinusoidally. Therefore, VIV has been studied by many researchers. Liu (1998) studied numerically hydrodynamic coefficients for fixed and oscillating cylinders. An experiment on VIV at a low Reynolds number was conducted by Anagnostopoulos (1992), who showed that the maximum oscillation amplitude occurs near the lower limit of the lock-in region at Re = 115. Kara

*[1]Corresponding Author, Email: wgpark@pusan.ac.kr,

(2012) performed numerical studies for comparison with experimental results (Anagnostopoulos, 1992). A numerical analysis of the dynamic behavior of a two-cylinder array was conducted by Derakhshandeh (2012). In addition, Qu (2009) studied a 2-DOF (Degree Of Freedom) three-cylinder array that had a regular triangular arrangement but with changes in the length.

In the present study, we conduct a CFD simulation of the dynamic response caused by an array of cylinders under the condition of a low Reynolds number. First, a stationary cylinder is investigated to find the hydrodynamic coefficient at a low Reynolds number. Then, the cylinder is free to oscillate with multiple degrees of freedom in a uniform flow. The motion of the cylinder is modeled using a damped degree of freedom system

2. Numerical Method

2.1 Mathematical model

A mass-damping-spring system is used as a dynamic behavior model of a cylinder. Figure 1 shows a schematic of the mass-damping-spring system used for the cylinder.

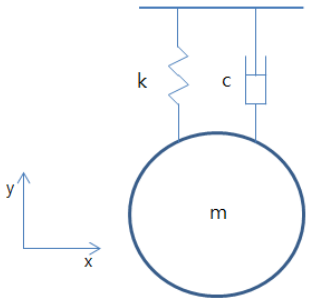

Fig. 1. Schematic of cylinder vibration

$$m\ddot{y} + c\dot{y} + ky = F(t) \qquad (1)$$

In the equation above, m is the mass of the system, y is the normal direction of flow, $\dot{y}$ is the velocity of the cylinder; $\ddot{y}$ is the acceleration of the cylinder; c is the damping coefficient, k is the spring stiffness, and $F(t)$ is the external force exerted on the cylinder. Equation 1 is solved using the Newmark-β method, which is widely used in the numerical evaluation of the dynamic responses of structures and solids. In the Newmark-β method, coefficient β has various values between 0 and 1. If β is 0, the equation can be explicitly solved without iteration. It is set to 0 in the present study.

In the present study, a loosely coupled method is used for the fluid-structure interaction in the following process. First, the flow field is solved using a CFD code. The dynamic equation (Eq.1) is solved using the Newmark-β method based on the external force of the flow field. Then, the center of the cylinder is updated by using the dynamic layering method provided by ANSYS FLUENT (2010). The Newmark-β method and dynamic method are determined using a UDF (User Defined Function) provided by ANSYS FLUENT (2010).

2.2 Boundary condition and setup

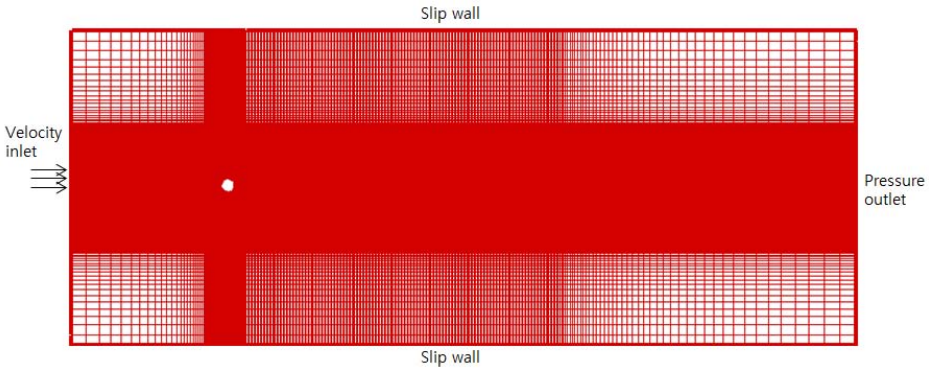

Fig. 2. Grid system and boundary condition

Figure 2 shows the computational domain and boundary condition. The computational domain is discretized to a structure grid. The grid number is approximately 341,000. To capture the boundary layer around the wall, the grid is clustered near the wall ($y^+ < 1$). The computational domain is extended to 10 diameters at the inlet and 50 diameters at the outlet. The left side is set as the velocity inlet, whereas the right side is set as the pressure outlet, and the upper and lower walls are set as slip walls.

The CFD calculations shown here are based on simulated solutions to the incompressible Navier-Stokes equation, carried out using ANSYS FLUENT v.13. Pressure-velocity coupling for an incompressible flow is used for SIMPLE (semi-implicit method for pressure-linked equations). This method was defined by Patankar (1972). The momentum discretization uses the QUICK (Quadratic Upwind Interpolation for Convection Kinetics) scheme.

3. Result and discussion

3.1 Stationary motion

Prior to the dynamic behavior analysis, a stationary cylinder is investigated to find the hydrodynamic coefficient at a low Reynolds number. The numerical results are compared to experimental results found by Liu (1998).

Table 1 Hydrodynamic coefficient and Strouhal number at Re = 200

	C_D	C_L	S_t
Exp.	1.3	-	1.9
Present	1.345 ± 0.04	± 0.62	0.202

For the drag coefficient and Strouhal number, the numerical results show good agreement with the experimental results. Figure 3 shows the contour of the flow and the force coefficients. Figures 3 (a), (b), and (c) illustrate the Karman vortex at a low

Reynolds number. Because of the flow separation, the results for an unsteady flow show alternating separation of the vortices. Figure 3 (d) shows the drag and lift coefficients over time. This figure shows that the frequency of the lift coefficient is twice that of the drag coefficient. This is because the amplitude of the lift coefficient changes on the positive and negative sides of the axis (Kara, 2012). Next, the Strouhal number of the wake is compared to the value obtained in experimental results at a low Reynolds number. The numerical results show good agreement with the experimental results.

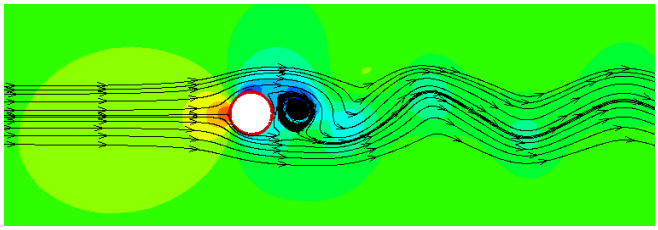

(a) Pressure distribution and streamlines

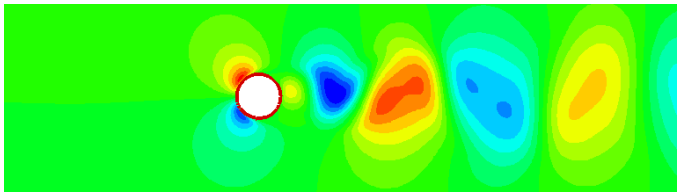

(b) y-velocity contour

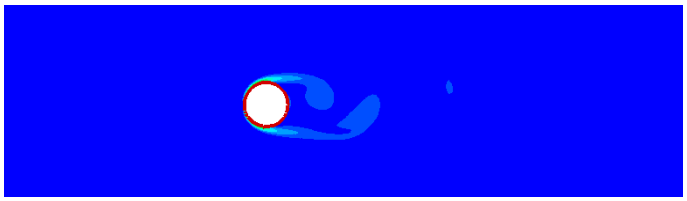

(c) Vorticity contour

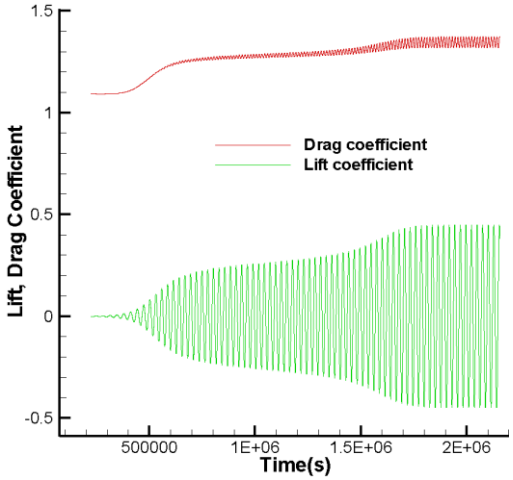

(d) Lift and drag coefficient

Fig. 3. Pressure, velocity, vorticity contour, and force coefficients

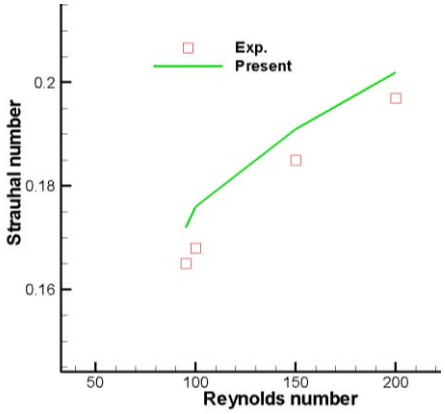

Fig. 4. Strouhal number in terms of Reynolds number

3.2 Dynamic motion

Next, the dynamic behavior of a cylinder is studied using a coupled method. The cylinder is free to oscillate with multiple degrees of freedom in a uniform flow. The motion of the cylinder is modeled using a damped degree of freedom system. Information about the structure and fluid is provided by Anagnostopoulos (1992). The diameter (D) and mass of the cylinder are 0.0016 m and 35.78 g, respectively. The spring stiffness is 69.48 kN/m, the damping coefficient is 0.0039 Ns/m, and the length of the cylinder is 0.1185 m. The distance between cylinders is 2.5 D. Figure 5 shows the pressure distribution and streamline for two cylinders. The front cylinder causes a vortex. Because of this vortex, the amplitude of the rear cylinder is extended in a direction normal to the inflow direction. Figure 6 shows the center points and lift coefficients of the cylinders. The center point of the rear cylinder is larger than the center point of the front cylinder. Moreover, Figure 6 shows that the lift coefficient increases as the amplitude of the rear cylinder increases.

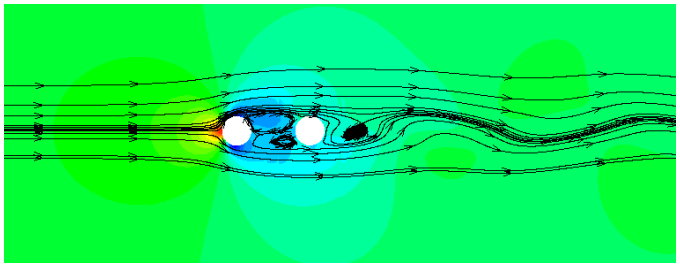

Fig. 5. Pressure distribution and streamlines

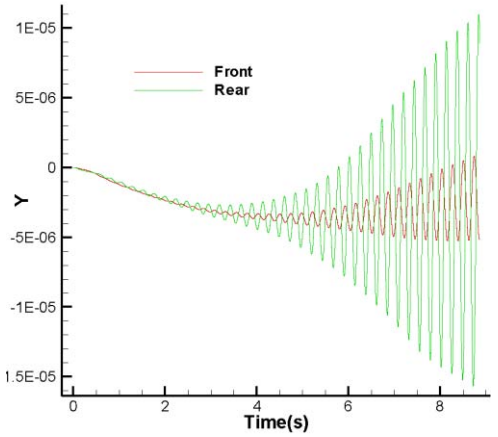

(a) Transverse oscillation of cylinder

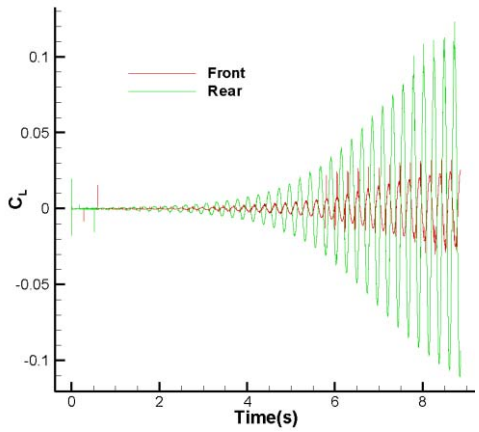

(b) Lift coefficient

4. Conclusion

In the study, the drag coefficient of a single cylinder was compared to the value obtained in experimental results when the Reynolds number was 200. In addition, the Strouhal number was compared to the value obtained in experimental results, but with a change in the Reynolds number. Next, investigations were conducted for cylinders arranged in a series. The center-to-center distance between two cylinders was 2.5 D.

Because of the vortex generated, the amplitude of the rear cylinder was extended in a direction normal to the inflow direction. The next study will investigate the dynamic behavior and hydrodynamic coefficient, but with a change in the distance between two cylinders.

ACKNOWLEDGMENT

This work was supported by the Human Resources Development of the Korea Institute of Energy Technology Evaluation and Planning (KETEP) grant funded by the Korea Government Ministry of Knowledge Economy (No. 20114010203080).

REFERENCES

Kara, M. and Stoesser, T. (2012), "A numerical method to predict fluid-structure interaction of flow past an elastically mounted circular cylinder", Proceedings of '2012 ISOPE Conference, Rhodes, Greece.

Liu, C., Zheng, X. and Sung, C.H. (1998), "Preconditioned multigrid methods for unsteady incompressible flows." *Journal of Computational Physics,* Vol. 139(35), pp. 35-57.

Ou, J.P., Xu, F. and Xiao, Y.Q. (2009). “Numerical simulation of Vortex Induced Vibration of three cylinders in regular triangle arrangement”, 2009 The Seventh Asia-Pacific Conference, Taipei, Taiwan.

ANSYS FLUENT User’s Guide. (2010)

Yang, J., Preidikman, S. and Balaras, E. (2008), "A strongly coupled, embedded-boundary method for fluid-structure interactions of elastically mounted rigid bodies." *Journal of Fluids and Structures,* Vol. 24, 167-182.

Patankar, S.V. and Spalding, D.B. (1972), “A Calculation procedure for heat, mass and momentum transfer in three-dimensional parabolic flows”, *International Journal of Heat and Mass Transfer*, Vol. 15, pp. 1787.

Anagnostopoulos, P. and Bearman, P.W. (1992), “Response characteristics of a vortex-excited cylinder at a low Reynolds number”, *Journal of Fluids and Structures*, Vol. 6, pp. 39-50.

Derakhshandeh, J.F., Arjomandi, M., Cazzolato, B. and Dally, B. (2012). “Numerical simulation of vortex-Induced vibration of elastic cylinder”, 18th Australasian Fluid Mechanics Conference, Launceston, Australia.

Hashamdar, H., Ibrahim, Z. and Jamel, M. (2011). “Finite element analysis of nonlinear structures with Newmark method”, *International Journal of the Physical Sciences*, Vol. 6(6), pp. 1395-1403.